submitted to ApJ Letter

General Relativistic Radiative Transfer and General Relativistic MHD Simulations of Accretion and Outflows of Black Holes

Steven V. Fuerst[1], Yosuke Mizuno[2,5], Ken-Ichi Nishikawa[2,3] and Kinwah Wu[4]

ABSTRACT

We calculate the emission from relativistic flows in black hole systems using a fully general relativistic radiative transfer formulation, with flow structures obtained by general relativistic magneto-hydrodynamic simulations. We consider thermal free-free emission and thermal synchrotron emission. Bright filament-like features protrude (visually) from the accretion disk surface, which are enhancements of synchrotron emission where the magnetic field roughly aligns with the line-of-sight in the co-moving frame. The features move back and forth as the accretion flow evolves, but their visibility and morphology are robust. We propose that variations and drifts of the features produce certain X-ray quasi-periodic oscillations (QPOs) observed in black-hole X-ray binaries.

Subject headings: accretion, accretion disks, jets — Kerr black hole physics — X-rays: binaries

1. Introduction

Relativistic jets are ubiquitous in accreting systems: active galactic nuclei (AGNs) (e.g. Urry & Pavovani 1995; Ferrari 1998; Blandford 2002), microquasars (e.g. Mirabel & Rodriguez 1999) and neutron-star X-ray binaries (e.g. Fender et al. 2004). They are believed

[1]Kavli Institute for Particle Astrophysics and Cosmology, Stanford, CA 94304

[2]National Space Science and Technology Center, 320 Sparkman Drive, Huntsville, AL 35805

[3]Center for Space Plasma and Aeronomic Research, University of Alabama in Huntsville

[4]Mullard Space Science Laboratory, University College London, Holmbury St. Mary, Surrey RH5 6NT, UK

[5]NASA Postdoctoral Program Fellow, NASA Marshall Space Flight Center

to emerge from the innermost regions of the accretion disks where the disk interfaces with the compact object (Meier, Koide, & Uchida 2001). Mechanisms proposed for relativistic-jet formation generally involve acceleration from the accretion disk driven by either magneto-hydrodynamic centrifugal force or magnetic pressure, (e.g. Blandford & Payne 1982), or by extracting rotational energy from the compact object (in the case of rapidly rotating black holes) (Penrose 1969; Blandford & Znajek 1977). However, the disk-jet coupling mechanism in black-hole systems is still a fundamental astrophysics question demanding an answer. Studies of accretion disks/tori and their outflow, have employed general relativistic magneto-hydrodyanmics (GRMHD) simulations (e.g. Koide et al. 1998, 1999, 2000; De Villiers et al. 2003, 2005; McKinney & Gammie 2004; McKinney 2006; Nishikawa et al. 2005a, 2005b; Hawley & Krolik 2006). Recently, radiative transfer calculations have modelled the emission from the structures determined by the GRMHD simulations (Schnittman & Rezzola 2005; Schnittman et al. 2006). These studies demonstrated that variability of emission can be caused by structural variations in the accretion disks, and quasi-periodic oscillations (QPOs) are a manifestation of such variations.

This work concerns the emission properties from relativistic flows near black holes, with the inclusion of the effects due to magnetic fields, which are important components in black-hole accretion (see Ji et al. 2006). In the accretion, inflows and outflow (jets) are determined by GRMHD simulations (following Mizuno et al. (2006b)) of jet formation from accretion disks. The radiations from the flows are calculated via the radiation transfer formulation described in Fuerst & Wu (2004).

§2 and §3 describe our GRMHD simulation of jet formation and general relativistic radiative transfer calculations respectively. §4 presents the results of the calculations; §5 discusses the astrophysical implications.

2. General Relativistic MHD Simulations

We consider a jet launched from an initially geometrically thin Keplerian disk around a rotating black hole (Mizuno et al. 2006b). The 3-dimensional GRMHD code "RAISHIN" (Mizuno et al. 2006a) is set to a 2.5-dimensional geometry in our simulations. We assume axi-symmetry with respect to the z-axis and mirror symmetry with respect to the equatorial plane. The Fiducial Observer (FIDO) coordinates are used, with the $3+1$ formalism for the Maxwell equations, Ohm's law (with no electrical resistance, i.e. ideal MHD condition) and conservation of particle number and energy-momentum on a curved spacetime (Mizuno et al. 2006a). Radiative pressure is omitted. The simulations are carried out in a spatial region with $0.75\ r_{\rm s} \leq r \leq 20\ r_{\rm s}$ and $0.03 \leq \theta \leq \pi/2$ (where $r_{\rm s}$ is the Schwarzschild radius), which is

divided into 128×128 zones, with logarithmic radial zone-spacing. Fluids, magnetic fields and waves are allowed to pass freely through the inner and outer boundaries (of the radial direction).

At the start of each simulation run the accretion disk is Keplerian, is penetrated by a uniform magnetic field, and rotates in a prograde direction with respect to the black hole. The background matter is in a corona free-falling into the black hole (i.e. Bondi-type flow). The density of the disk matter is about 100 times higher than the ambient matter. The black-hole spin parameter is $a = 0.95$.

The angular momentum of the disk is transported outward via magnetic stress. Matter exiting through the outer boundary of the simulation is replenished by the inflow from the outer accretion disk. As the simulation proceeds, matter flows in because of angular-momentum loss. The inflowing matter encounters a centrifugal barrier at about $r = 2\ r_{\rm s}$, where a shock is formed. The gas pressure increases at the shock, and the ionised gas near the shock is accelerated by the Lorentz force, leading to an outflow (jet) (see Fig. 1b). At the same time, rotational frame-dragging by the black hole twists the magnetic field and generates an additional outflow component. This component is faster and more collimated than the spatially extensive, slower component accelerated by the disk accretion flow alone (Mizuno et al. 2006b).

The duration of each simulation is typically $t = 200\ t_{\rm s}$, where $t_{\rm s} = r_{\rm s}/c$. The flow density, pressure and velocity, and the magnetic field obtained by the simulation are written out at intervals of $\Delta t = 5\ t_{\rm s}$. The hydrodynamic variables and the magnetic field are normalised with respect to scale-free quantity ρ_0. For radiative transfer calculations, we adopt the following conversion for the density, pressure and magnetic field (in c.g.s. units): $\rho = \rho_0 \rho_{\rm hd}$, $P = \rho_0 c^2 P_{\rm hd}$, and $B = \sqrt{8\pi\rho_0 c^2} B_{\rm hd}$. We set $\rho_0 = 10^{12}$ protons cm^{-3}, which gives comparable strengths for the synchrotron and free-free emission processes (see §3). For the length normalization, we set $r_{\rm s} = 2 \times 10^{11}$ cm.

3. General Relativistic Radiative Transfer

The relativistic radiative transfer equation (in a split-frame form) reads

$$\frac{\partial \mathcal{I}(\nu_\infty)}{\partial \lambda} = \gamma^{-1} \left[-\chi_0(\nu_0) \mathcal{I}(\nu_\infty) + \mathcal{J}_0(\nu_0) \right] \ , \tag{1}$$

where $\mathcal{I}$ the Lorentz-invariant intensity, χ_0 and $\mathcal{J}_0$ are the Lorentz-invariant absorption and emission coefficients respectively, and λ is the affine parameter. The relative energy shift of the photon between the observer's frame at infinity and the comoving frame is

$\gamma = -E_\infty/k_\alpha u^\alpha = \nu_\infty/\nu_0$, where k_α is the four momentum of the photon, and u^α is the four velocity of the medium. The transfer equation may be written as:

$$\frac{\partial \tau}{\partial \lambda} = \gamma^{-1}\chi_0 \; ; \tag{2}$$

$$\frac{\partial \mathcal{I}_{\rm final}}{\partial \lambda} = \gamma^{-1}\mathcal{J}_0 e^{-\tau(\lambda)} \; . \tag{3}$$

where $\mathcal{I}_{\rm final}$ is the intensity of an observed ray which starts at λ with zero intensity, and

$$\tau(\nu_\infty) = \int \gamma^{-1}\chi_0(\nu_\infty/\gamma)d\lambda \; . \tag{4}$$

We consider thermal synchrotron emission (Wardziński & Zdziarski 2000) and thermal free-free emission. We assume the matter is ionized hydrogen, and the Gaunt factor is unity. (The conclusions will not differ qualitatively if other values of metallicity and Gaunt factor are used.)

The radiative transfer equation is solved via backward ray-tracing. We render images of the disks and outflows, with each pixel yielding a spectrum. Equations (2) & (3) are evaluated for every energy bin. We use N energy bins, and there are $2N + 6$ coupled differential equations to solve on each step along the ray, where the 6 additional equations are for the ray path. We use a 4th-order Runge-Kutta Cash-Karp algorithm for the integrations. The ray-path equations are solved to a numerical accuracy of one part in 10^{11}, and the intensity and optical depth equations to one part in 10^7.

4. Emission from Accretion and Outflows

Figures 2a, b and c show emission from the lensed disk and the outflow/jet at various viewing inclinations θ and simulation times t. The usual bright inner ring (corresponding to the first-order lensed disk image) is clearly visible in the images. An additional new ring develops as the simulation proceeds (cf. Fig. 2a and b). This ring is due to thermal free-free emission from the dense hot gas in the innermost region of the accretion disk, where the bipolar outflows/jets are launched. Its image is distorted by gravitational lensing, and its intensity is severely modified by time dilation and Doppler boost.

The emission of the outflow/jets is almost invisible at low and medium view inclinations ($\theta < 45^\circ$), because of the bright background emission from the accretion disk, which has much higher density than the jets. However, it becomes slightly more visible at higher viewing inclinations. In the optically thin case ($\theta = 85^\circ$, Fig. 2c), the jet is still much fainter than

the accretion disk, but the brightest magnetic knots in the counter jet are visible. The thermal free-free emission ring is visible, as in the $\theta = 45^\circ$ case. When we set the emission to be optically thick to Thomson scattering, the two-component jets (see §2) become visible (Fig. 2d). The magnetic field in the inner jet is strongly twisted by frame-dragging by the rotating black hole. As the field is wound up, it is compressed, and strong synchrotron emission produces clear jet structures. The twisting of the magnetic fields in the outer jet is mainly due to disk rotation and field compression is less severe. This gives weaker synchrotron emission.

A completely unexpected outcome is the formation of bright filament-like features above the disk surface. They were enhanced synchrotron emission caused by chance alignment of the magnetic field in the gas rest frame to the line-of-sight. In this viewing orientation, the synchrotron emission is strongly boosted. As the simulation progresses, the variation of the direction of the magnetic field causes these filament features to wiggle and to sweep across the disk. This changes the integrated intensity. These features are robust, and are visible throughout the simulation at all viewing inclinations. The oscillations of these filaments occur on certain timescales but they are not strictly periodic, i.e. QPOs.

5. Discussions and Summary

High-frequency X-ray QPOs are observed in a number of black-hole X-ray binaries, e.g. GRO J1655−40 (Strohmayer 2001). The QPO frequencies are close to the rotational frequency of the last stable circular particle orbit, indicating a relativistic origin. In spite of great efforts (e.g. Nowak et al. 1997; Rezolla et al. 2003), the mechanisms leading to these QPOs are yet to be clarified. Some recent works (e.g. Schnittman & Rezzolla 2006) considered numerical hydrodynamic simulations incorporating with radiative transfer in fully relativistic framework. They attribute the QPOs to the density variations in the flows, via the presence of a hot or dense blob in the accretion disk orbiting very close to the black hole, or the oscillations of the accretion disk itself.

Our calculations show that QPOs could be of radiative and magnetic origin, in the setting where strong gravity causes lensing, rotation of the black hole induces frame dragging, and shear of the flows winds the magnetic field. The filament-like features near the accretion disk may be sites where X-ray QPOs are generated. We argue that the QPO X-rays are probably not due to direct synchrotron emission. Instead, they are emission produced by inverse Compton scattering of ambient low-energy photons by fast streaming electrons along the magnetic field lines, i.e. the energetic electrons that produce the boost synchrotron radiation filaments. The photons scattered into the line-of-sight by the field-aligned stream-

ing electrons are of the highest energy and are most strongly Doppler boosted. Photons scattered into the line-of-sight from electrons following field lines in other directions are less boosted, and do not have temporal signatures as clear as those scattered by the line-of-sight field-aligned streaming electrons. The robustness of the filament features in the image implies that the QPO's generated by the process are also robust. This model has an advantage over the conventional circulating-blob scenario in that the strong shear in the flows will not suppress QPOs but, in contrast, may reenforce QPOs by sustaining the magnetic field winding process, which is essential in the scenario.

In summary, we have conducted GRMHD and general relativistic radiation transfer calculations of accretion flows and outflows/jets in black-hole systems. We have demonstrated that accretion not only leads to jet formation but also strong twisting and winding of the magnetic field. While the direct emission from the jet components may be overwhelmed by the disk emission, the topology and properties of the magnetic fields in the jet could have significant observational consequences. Our calculations show that robust filament-like bright features can occur when the magnetic fields are roughly aligned with lines-of-sight. These features are not stationary but oscillate quasi-periodically. At the locations of these features, synchrotron emission from the fast-streaming electrons along the field lines are strongly boosted. Moreover, photons that are inversely Compton scattered into the line-of-sight by these field-aligned streaming electrons are also strongly boosted and retain the temporary signatures of the filaments. Thus, we provide a viable QPO scenario in which simple changes in the local magnetic field orientations, together with gravitational light bending, are sufficient to produce observable X-ray variability. Future GRMHD simulations of longer duration will produce light curves that enable the construction of power density spectra and hence verify this QPO scenario.

Y.M. is a NASA Postdoctoral Program fellow at NASA-MSFC. K.N. is supported by the NSF awards ATM-0100997, INT-9981508 and AST-0506719, and the NASA award NNG05GK73G to UAH. The simulations were performed on an IBM p690 (Copper) at NCSA, supported by NSF.

REFERENCES

Blandford, R. D. 2002, in *Lighthouses of the Universe*, eds. M. Gilfanov, R. Sunyaev et al., Springer, Berlin, p206

Blandford, R. D. & Znajek, R. L. 1977, MNRAS, 179, 433

Blandford, R. D. & Payne, D. G. 1982, MNRAS, 199, 883

De Villiers, J.-P., Hawley, J. F. & Krolik, J. H. 2003, ApJ, 599, 1238

De Villiers, J.-P., Hawley, J. F., Krolik, J. H. & Hirose, S. 2005, ApJ, 620, 878

Fender, R., Wu, K., Johnston, H., Tzioumis, T., Jonker, P., Spencer, R., van der Klis, M., 2004, Nature, 427, 222

Ferrari, A. 1998, ARA&A, 36, 539

Fuerst, S. V. & Wu, K. 2004, A&A, 424, 733

Hawley, J. F. & Krolik, J. H. 2006, ApJ, 641, 103

Ji, H., Burin, M., Schartman, E. & Goodman, J. 2006, Nature, 444, 343

Koide, S., Shibata, K. & Kudoh, T. 1998, ApJ, 495, L63

Koide, S., Shibata, K. & Kudoh, T. 1999, ApJ, 1999, 522, 727

Koide, S., Meier, D. L. Shibata, K. & Kudoh, T. 2000, ApJ, 536, 668

McKinney, J. C. 2006, MNRAS, 368, 1561

McKinney, J. C. & Gammie, C. F. 2004, ApJ, 611, 977

Meier, D. L. Koide, S. & Uchida, Y. 2001, Science, 291, 84

Mirabel, I. F. & Rodríguez, L. F. 1999, ARA&A, 37, 409

Mizuno, Y., Nishikawa, K.-I., Koide, S., Hardee, P., & Fishman, G. J. 2006a, ApJS, submitted, (astro-ph/0609004)

Mizuno, Y., Nishikawa, K.-I., Koide, S., Hardee, P., & Fishman, G. J. 2006b, ApJ, submitted, (astro-ph/0609344)

Nishikawa, K.-I. Richardson, G., Koide, S., Shibata, K. Kudoh, K., Hardee, P. & Fishman, G. J. 2005, ApJ, 625, 60

Nishikawa, K.-I., Mizuno, Y., Fuerst, S., Wu, K., Richardson, G., Sol, H., Koide, S., Shibata, K., Kudoh, T. & Fishman, G. J. 2005, in Proceeding of Astrophysical Sources of High Energy Particles and Radiation, eds. T. Bulik, B. Rudak, G. Madejski, AIP Conf. Proc., 801, p184 (astro-ph/0509601)

Nowak, M. A., Wagoner, R. V., Begelman, M. C., Lehr, D. 1997, ApJ, 477, L91

Penrose, R., 1969, Rev. Nuovo Cimento, 1, 252

Rozella, L., Yoshida, S., Maccarone, T. J., Zanotti. O. 2003, MNRAS, 344, L37

Schnittman, J. D. & Rezzolla, L. 2006, ApJ, 637, L113

Schnittman, J. D., Krolik, & Hawley, J. F. 2006, ApJ, 651, 1031

Strohmayer, T. E., 2001, ApJ, 552, L49

Urry, C. M. & Padovani, P. 1995, PASP, 107, 903

Wardziński, G., G., Zdziarski A. A. 2000, MNRAS, 314, 183

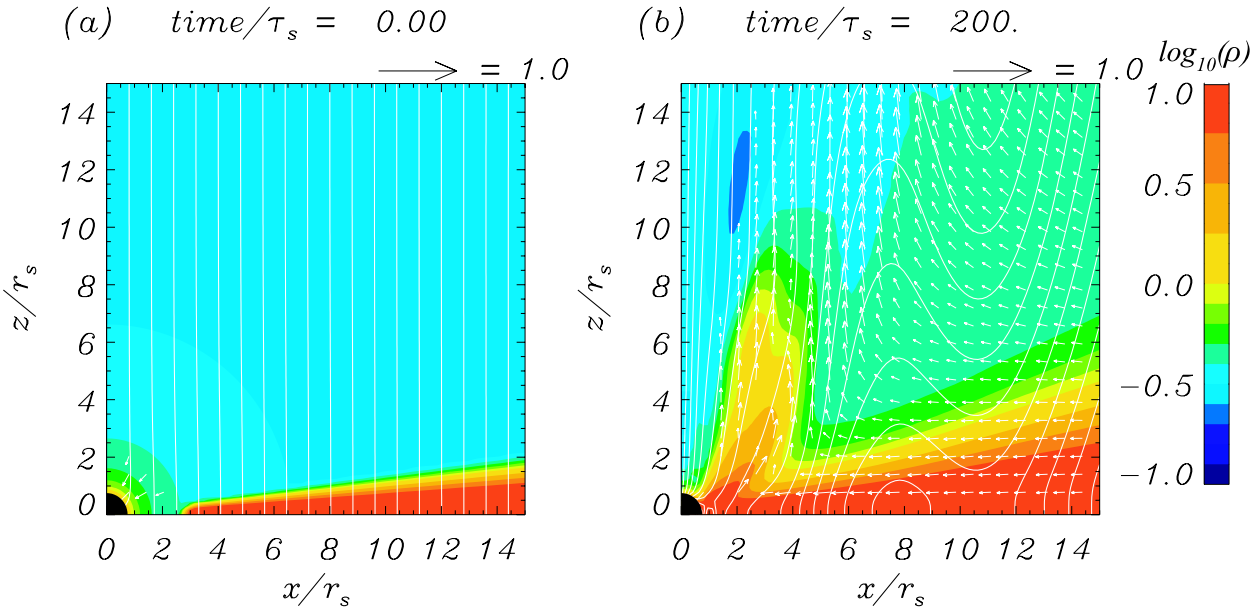

Fig. 1.— Snapshots of proper density of the accretion inflow and outflow obtained by the GRMHD simulation at $t/t_{\rm s} = 0$ and 200. The white curves represent magnetic field lines (contours of poloidal vector potential) and the arrows depict the poloidal velocities normalized to the speed of light.

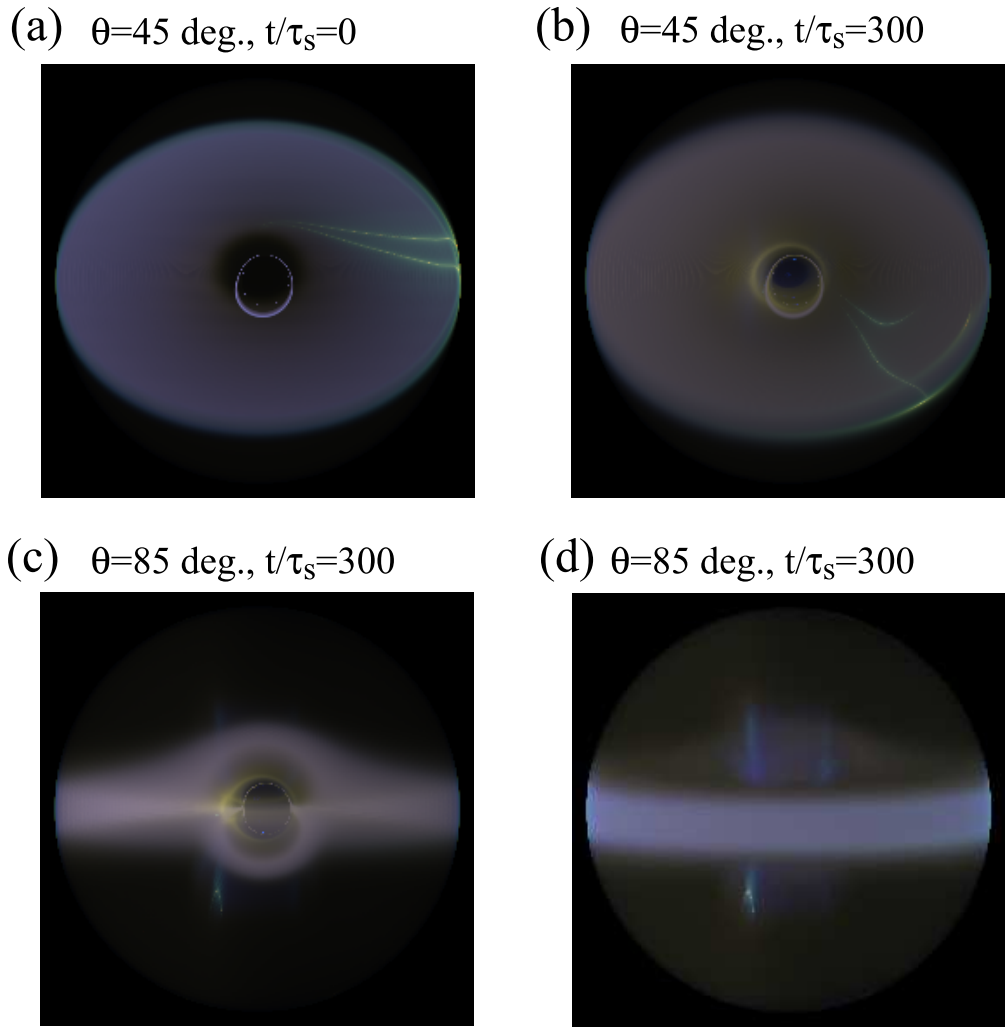

Fig. 2.— *Top:* Images of emission from the simulated flows viewed at an inclination angle of 45° at $t/t_{\rm s} = 0$ and 300, corresponding to the initial and final states of the simulation respectively. The jet is invisible, but bright synchrotron filaments can be seen near the disk surface. The bright blue ring at the center is a first-order lensed disk image, as light orbits the black hole on its way to the observer. A new fuzzy yellowish ring appears near the center of the image of $t/t_{\rm s} = 300$. It corresponds to the direct thermal free-free emission from highly dense gas piled up in the inner accretion disk. *Bottom:* Images of emission from flows viewed at an inclination angle of 85° for optically thin and optically thick cases (panels c and d respectively). For the optically thick case, we consider an additional opacity due to Thomson scattering. We approximate this process by assuming that it only removes the line-of-sight photons without adding photons into the line-of-sight substantially. As the thermal synchrotron and the thermal free-free emission are both optically thin, the absorptive opacity is provided by Thomson scattering. The counter-jet is visible below the equatorial plane in the optically thin case. The details of the jet are more visible in the optically thick case.